Liu, Xuwen; Haimi, Eero; Hannula, Simo-Pekka; Ylivaara, Oili M. E.; Puurunen, Riikka L.

On the reliability of nanoindentation hardness of Al2O3 films grown on Si-wafer by atomic layer deposition

Published in:
JOURNAL OF VACUUM SCIENCE AND TECHNOLOGY A

DOI:
10.1116/1.4842655

Published: 01/01/2014

Document Version
Publisher's PDF, also known as Version of record

On the reliability of nanoindentation hardness of Al_2O_3 films grown on Si-wafer by atomic layer deposition

Xuwen Liu, Eero Haimi, Simo-Pekka Hannula, Oili M. E. Ylivaara, and Riikka L. Puurunen

Citation: Journal of Vacuum Science & Technology A **32**, 01A116 (2014); doi: 10.1116/1.4842655
View online: https://doi.org/10.1116/1.4842655
View Table of Contents: http://avs.scitation.org/toc/jva/32/1
Published by the American Vacuum Society

On the reliability of nanoindentation hardness of Al_2O_3 films grown on Si-wafer by atomic layer deposition

Xuwen Liu,[a] Eero Haimi, and Simo-Pekka Hannula
Department of Materials Science and Engineering, Aalto University School of Chemical Technology, Vuorimiehentie 2A, FI-00076 Espoo, Finland

Oili M. E. Ylivaara and Riikka L. Puurunen
VTT Technical Research Centre of Finland, Tietotie 3, FI-02044 Espoo, Finland

(Received 2 September 2013; accepted 22 November 2013; published 11 December 2013)

The interest in applying thin films on Si-wafer substrate for microelectromechanical systems devices by using atomic layer deposition (ALD) has raised the demand on reliable mechanical property data of the films. This study aims to find a quick method for obtaining nanoindentation hardness of thin films on silicon with improved reliability. This is achieved by ensuring that the film hardness is determined under the condition that no plastic deformation occurs in the substrate. In the study, ALD Al_2O_3 films having thickness varying from 10 to 600 nm were deposited on a single-side polished silicon wafer at 300 °C. A sharp cube-corner indenter was used for the nanoindentation measurements. A thorough study on the Si-wafer reference revealed that at a specific contact depth of about 8 nm the wafer deformation in loading transferred from elastic to elastic–plastic state. Furthermore, the occurrence of this transition was associated with a sharp increase of the power-law exponent, m, when the unloading data were fitted to a power-law relation. Since m is only slightly material dependent and should fall between 1.2 and 1.6 for different indenter geometry having elastic contact to common materials, it is proposed that the high m values are the results from the inelastic events during unloading. This inelasticity is linked to phase transformations during pressure releasing, a unique phenomenon widely observed in single crystal silicon. Therefore, it is concluded that m could be used to monitor the mechanical state of the Si substrate when the whole coating system is loaded. A suggested indentation depth range can then be assigned to each film thickness to provide guidelines for obtaining reliable property data. The results show good consistence for films thicker than 20 nm and the nanoindentation hardness is about 11 GPa independent of film thickness.
[http://dx.doi.org/10.1116/1.4842655]

I. INTRODUCTION

Atomic layer deposition (ALD) is a thin film deposition method belonging to the general class of chemical vapour deposition methods. ALD operates by exposing a solid surface alternately to reactive gaseous chemicals, the exposures being separated by purge/evacuation.[1–3] The self-terminating reaction chemistry makes ALD films exceptionally uniform in thickness, irrespective of surface shape, and even highly complex 3-D structures can be conformably coated. The processes are known also as robust and reproducible. As a consequence, there is rising interest toward ALD in many industrial sectors (e.g., microelectronics and paper) as well as in highly versatile research and development an area (e.g., catalysis, nanostructures, and nanoelectronics).

One sector, where ALD is seen as one of the future technologies, is microelectromechanical systems (MEMS). The major benefit of ALD for MEMS is the combination of low deposition temperatures (often <300 °C) with conformal coatings that is not achieved by conventional fabrication technologies.[4] Mechanical properties are crucial for the function of MEMS devices. For example, elastic modulus directly influences the resonating frequency of MEMS cantilevers. In general, mechanical properties such as elastic modulus, hardness, fracture toughness, and Poisson's ratio are needed as input parameters when modelling MEMS structures with ALD layers.

From a recently published overview on ALD,[3] it appears that the majority of the research work has been focused either on the basics of the ALD process or on its industrial applications, especially in microelectronics. In comparison, much less studies have been devoted to the mechanical behavior of ALD films under external loading.[5–10] Most of the mechanical characterization has been done on Al_2O_3, HfO_2, and TiO_2 thin film systems on silicon substrate by instrumented nanoindentation. The limited information found in literature presents uncertainties in assessing the mechanical behavior of thin ALD films. For example, the reported hardness values of ALD Al_2O_3 films are scattered between 6 and 12 GPa.[5–8] In the studies, the deposition temperature apparently has an influence on this variation but not in a consistent way. Therefore, the hardness variation does not necessarily reflect the intrinsic film property change. Other factors including nanoindentation setup and data analysis must be accounted for in order to understand the mechanical response of the films. A recent study[11] highlights the reliability issue of nanoindentation data on ALD Al_2O_3 films. It concludes that the hardness of ALD Al_2O_3 films on

[a]Electronic mail: xuwen.liu@aalto.fi

a stiff substrate (e.g., silicon and glass) can be reliably obtained providing sufficient data can be selected for extrapolation. The standard procedure requires a linear extrapolation, which generally means that only low penetration data should be used to obtain reliable information on coating properties. This limitation imparts even more difficulties when thin films are to be characterized. This is because at shallow indent depths the indentation size effect (ISE), the inaccurate indenter area function, and the high noise-to-data ratio as well as the surface roughness all make valid data for extrapolation limited.

Nanoindentation has been widely used to characterize the mechanical properties of film/substrate systems due to its convenience, high efficiency, and inexpensiveness. In this technique, a depth-sensing instrument having a subnanometer resolution is used to indent into sample surface. The mechanical properties of the indented material can be extracted from a series of load versus depth data. An indirect method based on the knowledge of penetration depths and tip geometry is used to estimate the area of contact at peak load, from which the mean contact pressure–hardness can be determined. The elastic modulus is estimated based on the unloading data, assuming that there is always some degree of recovery due to elastic strain relaxation.[12] One of the most commonly used methods in extracting elastic modulus and hardness is the Oliver and Pharr method.[13] According to this method, the unloading data are well-described by a power-law relation

$$P = \alpha(h - h_f)^m, \tag{1}$$

where P is the indentation load, h_f is the final displacement after complete unloading, and α and m are material constants. Moreover, according to Pharr's effective-indenter-shape concept,[14] the power-law exponent, m, is only slightly material dependent and should fall between 1.2 and 1.6 for different indenter geometry having elastic contact to common materials. It has been stated[15] that $m > 2$ has no physical meaning since the corresponding effective indenter shape would be unrealistic. Large m values encountered in nanoindentation are often linked to inelastic events or reverse plasticity during unloading.

In characterization of film properties *via* nanoindentation method, it is common to restrict the indentation depth to a small fraction of film thickness, typically about 10%. For thin films (<100 nm), the applicability of this rule becomes problematic as the 10% restriction makes the indentation depth fall in the range where ISE, surface roughness as well as high noise-to-data ratio all complicate the results. Different methods have been developed to extract film-only property on systems having different types of film–substrate interactions. Several treatments[16–19] are based on Joslin and Oliver's idea[20] of utilizing the material characteristic of P/S^2. Here, P is the indentation load and S is the contact stiffness. For elastically homogeneous systems, hardness (H) and contact modulus (E_r) are usually constant with indent depth. It follows then P/S^2 should be also constant from the relation[21]

$$\frac{P}{S^2} = \frac{1}{\beta}\frac{\pi}{4}\frac{H}{E_r^2}. \tag{2}$$

For a film/substrate system, P/S^2 will vary depending on H and E of the film and substrate. Therefore, by plotting P/S^2 as a function of indentation depth one can have a more complete picture of the properties of an elastically mismatched film/substrate system. In general, all of the aforementioned treatments can, to some extent and with different accuracy, extract film elastic modulus from a corrected contact modulus by considering the contribution of the substrate. However, they all require that certain elastic properties of the film are separately determined when predicting the film-only hardness on either elastic homogeneous or elastic mismatched film-substrate systems. Moreover, all of them will fail when substrate yields. In a recent study,[22] an analytic model has been developed to extract substrate-independent modulus of thin films that work well for both compliant films on stiff substrates and stiff films on compliant substrates. However, it is not clear how this mode can be used in determining the film-only hardness since though the model can calculate the "true value" of the contact area through a sophisticated method by finite-element analysis, it is not specified in what deformation state the substrate is under the contact conditions. Therefore, there is no a ready solution that allows quick assessment of true film hardness. While, such a solution may be needed for ALD processed thin films on silicon not only for new film development but also for quality control and process re-engineering. It is often that the thin films' elastic property is unknown and processing parameter dependent.[22]

This study aims to find a quick method for obtaining nanoindentation hardness of thin films on silicon with improved reliability. Our work is not to develop a thorough solution covering all film–substrate systems, but an effort to draw attention on silicon based and ALD processed film systems, for single-crystal silicon is such an important substrate material for thin film systems in MEMS applications. The focus is placed on monitoring the deformation state of the substrate to ensure that no plastic deformation occurs in the substrate, which only provides an elastic support to a small fraction of the indenting loads. In addition to the importance of film property in modeling MEMS' structure, our special interests in obtaining reliable film hardness value are also originated from the correlation of contact resistance to tribological behavior of thin films[23] as the contact resistance can be indexed by the hardness to the contact modulus ratio in the form of H^3/E_r^2. Therefore, small changes in film hardness may result in large variations in its tribological performance. The ultimate film thicknesses that we are targeting are well under 100 nm, which are challenging for nanoindentation as the characterization technique.

II. EXPERIMENTAL METHODS

Aluminum oxide films were deposited on 150 mm p-type (001) silicon wafers by ALD. The single side polished (SSP) wafers were cleaned before deposition using RCA-cleaning (SC-1, hydrogen fluoride, and SC-2) and thus covered with

1–2 nm thick chemical oxide. The ALD reactor was a Picosun™ R-150. Precursors were trimethylaluminum Me_3Al and deionized water. The process pressure was about 5–30 bar with constant 200 sccm nitrogen flow through reactant lines. The pulse sequences for depositions were 0.1 s for reactions and 1 s for purges. The deposition temperature was at 300 °C, and film thickness was from 10 to 600 nm.

Nanoindentation measurements were carried out with a TriboIndenter® TI-900 (Hysitron, Inc.) nanomechanical testing system. The whole instrument set-up was fine-tuned to eliminate the mechanical, acoustic, and electric noise. The instrument was placed inside a semiclean room with constant laminar airflow to minimize the possible thermal drift during measurement. Indentations were performed under load-control mode with the loading, holding at peak-load and unloading segment time of 10, 5, and 5 s, respectively. The instrument stability and indentation repeatability were monitored by performing a series of 16 indents into a piece of Si wafer over a period of time with the peak load varying from 5 to 500 μN. This silicon piece was taken from the same wafer batch that was used as the substrate of the ALD Al_2O_3 films.

The mechanical response of the silicon wafer substrate was first investigated by carefully studying the characteristics of the initial part of the load-displacement plot and the variation of the power-law exponent, m, as a function of indent depth. In collecting m values, all of the indentation events were inspected at first to eliminate those for which the load-displacement curves were abnormally shaped and those for which excessive/reversed thermal drift were recorded. Then, unloading data in the range of 95–20% were used in the fitting. This way, it is expected that "m" would characterize all-and-only the mechanical responses occurring in the silicon during unloading. The investigation revealed a specific depth range, over which the corresponding m value experienced a sharp increase, indicating inelastic events occurred during unloading. Since the deformation was fully recoverable for indents made shallower than the specific depth, the sharp rise of m was linked to a transition of deformation state from pure elastic to elastic–plastic. Therefore, plastic deformation seemed to be a precondition for onset inelastic event in the silicon during unloading. It was then postulated that when the ALD coatings were measured there would be a similar sharp rise of m, but at deeper indent depths, provided that such inelastic events did not occur in the amorphous Al_2O_3. Consequently, this sharp rise of m would be a sign of inelastic events occurring solely in the substrate, which must be then in an elastic–plastic stage. Therefore, by monitoring the variation of m as a function of indent depth reliable hardness values that no plastic deformation occurs in the substrate could be obtained for the ALD films.

A cube-corner indenter with a 90° total include angle and a tip radius below 40 nm was used in the study. The idea of using a 90° shaped sharp indenter was to trigger the elastic to elastic–plastic transition at the vicinity of the silicon surface in order for any substrate effects being sensitively detected when thin films were applied. Our experiences tells that at large indent depths this tip shape might produce lower hardness values than those generated by a Berkovich tip on fused quartz, perhaps due to the large friction between the tip and the material. However, at a medium indent depth range up to 80 nm, the cube-corner tip gives good elastic modulus and hardness values on fused quartz as well as other materials. Moreover, previous works have also shown that the indenter sharpness and geometry can have a profound influence to the mechanical response of the uppermost surface layers in certain materials. In one study,[24] a cube-corner indenter is able to detect an ultrathin air-borne oxide layer on a low-k thin film. While in another study,[25] the same sharp tip induces an elastic to elastic–plastic transition in a single crystal alloy at the very beginning of indent. In both cases, the more commonly used Berkovich tip has either failed to identify the oxide layer or to induce the transition only at much deeper indent depths. The reason is that the sharp cube-corner indenter can generate much severer plastic strains in a more confined volume of material at the very top of the surface.

Throughout the measurement, the indenter conditions were checked regularly by indenting on the standard fused quartz to see if there were any changes of the tip rounding so that the area function needed a recalibration.

III. RESULTS AND DISCUSSION

A. Mechanical response of the silicon substrate reference

Repeated measurements on the Si-wafer reference revealed a highly reproducible pop-in phenomenon at a specific contact depth, about 8 nm—i.e., sudden excursion of indent depth occurred under constant load during loading. Figure 1 shows part of the loading curves from five indents performed at different times demonstrating that pop-ins occurred in each indent at a very similar depth. Previous studies[24,25] have ascribed the pop-in events either to the sudden failure of the air-borne oxide layer or to the transition of the deformation state from pure elastic to elastic-plastic. Pop-ins in nanoindentation may reflect homogeneous,

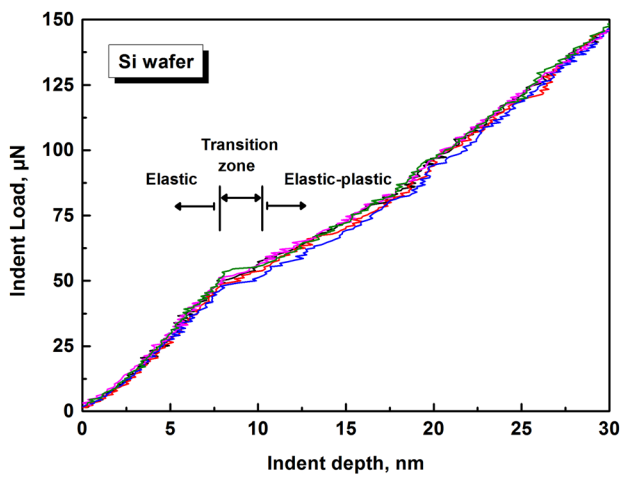

FIG. 1. (Color online) Overlaid plots of the loading curves from five indents on the film-free silicon wafer performed at different times.

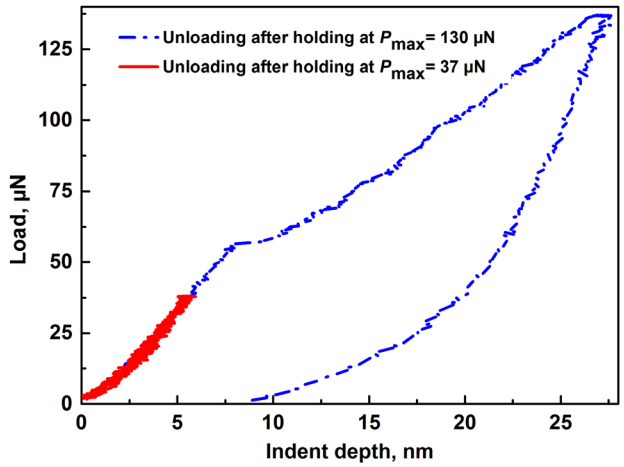

FIG. 2. (Color online) Unloading behavior of the film-free silicon wafer after withdrawal of tip from the elastic region and from the elastic-plastic region.

heterogeneous, or surface phenomena that can be linked ultimately to material plasticity at the upmost surface layers. For example, it has been found[26] that pop-in in nanoindentation of single crystal metals may be connected to homogeneous nucleation of glissile dislocation loops. The occurrence of the pop-in requires that the surface near the indenter has only a few if any dislocations so that the "defect-free" crystals will experience elastic deformation in the very beginning of loading. As one can see in Fig. 2, the indent depth was fully recovered when unloading (at the peak load of 37 μN) was made before the pop-in, while there was a clear residual depth when unloading was done after the pop-in (at a peak load of 130 μN). The conditions of the SSP silicon (SSP-Si) in this study seem to fit the transition explanation and it is likely that the observed pop-in (Fig. 1) in the film-free silicon correlates to the transition from pure elastic to elastic-plastic deformation. In Fig. 3, the load-displacement curves generated by a Berkovich tip and the sharp cube-corner indenter are compared. The cube-corner tip induced a pop-in at a contact depth of about 8 nm, while the Berkovich tip

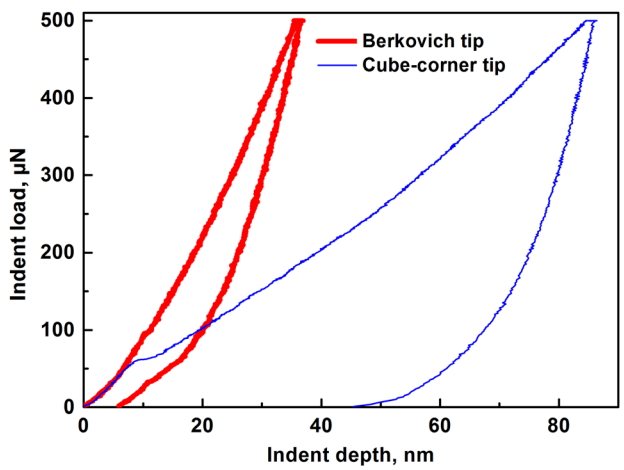

FIG. 3. (Color online) Characteristics of load vs indent depth plots generated by the sharp cube-corner tip and a Berkovich tip on the film-free silicon wafer.

TABLE I. Power-law exponent, m, at specific contact depths for the film-free silicon.

Contact depth (nm)	75.7–78.1	49.5–52.2	16.2–18.8	8.8–12.1	1.8–3.4
Power-low exponent (m)	3.2–3.6	2.8–3.8	2.6–3.5	2.3–3.0	1.2–1.6

resulted in a rather smooth and continuous curve with no clear depth excursion.

When fitting the unloading data to a power-law relation [Eq. (1)], it was found that the power-law exponent, m, sharply increased when loading into the elastic–plastic region (Table I). Each data range in Table I is established from the results of 16 indents made at each corresponding load at a different time. The small variations in contact depths are normal for indentations performed under load-control mode, depending on the instrument, environment, as well as local surface conditions. It is widely observed that in single crystal silicon phase transformations occur not only during pressurizing but also at pressure releasing.[27,28] Moreover, the transformations are associated with volume changes and are treated as inelastic events. Therefore, the sharp rise of m is likely to result from phase transformations occurring during unloading, a unique phenomenon found in single crystal silicon. In addition, the finding in this study suggests that a precondition for the onset of the inelastic events during unloading is the silicon being loaded to its elastic–plastic deformation stage.

B. Mechanical characterization of the ALD Al_2O_3 films

Figure 4 shows the power-law exponent, m, from indentation measurements to various contact depths of ALD Al_2O_3 films having various thicknesses on the silicon wafer substrate. For films thicker than 100 nm, all the m values fall in the range of 1.2–1.6. A critical value of contact-depth to film-thickness ratio is estimated as 0.85, corresponding to the second point on the 10 nm film curve in Fig. 4. Higher ratios than 0.85 leads to $m > 1.6$, indicating onset of inelastic events in the substrate during unloading. The 50 nm thick

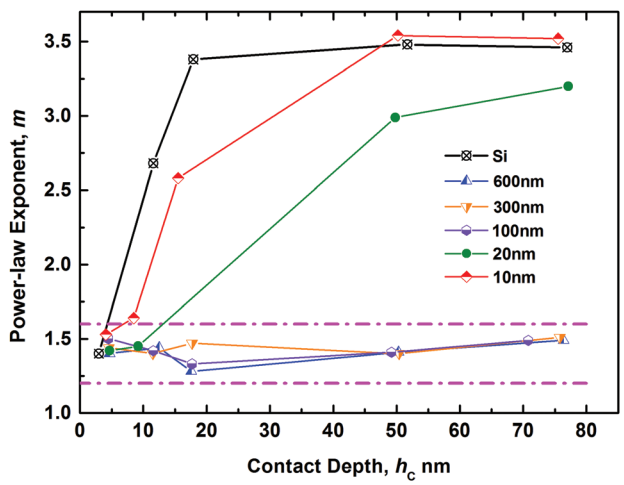

FIG. 4. (Color) Power-law exponent, m, as a function of contact depth for the ALD Al_2O_3 films of different thicknesses. Each point in the figure represents an average of nine indents.

film is an exception, for which m remains under 1.6 even when the contact-depth to film-thickness ratio is over 1.

The hardness at each specific contact depth is presented in Table II. The figures at each specific depth range in the table are the average of 16 indents. The figures in the gray-colored area are eliminated since the corresponding m values are larger than 2. As one can see, the hardness values are fairly constant over a large indent depth range for different film thicknesses. At the shallowest indent range (4.1–4.7 nm), the meaning of hardness is questionable since the plastic zone under the indenter was not fully developed (see Fig. 2). In addition, the inaccurate indenter area function due to bluntness, the surface roughness as well as the high noise-to-data ratio at shallow indents all make the data less reliable. However, for thicker than 20 nm films, it is rather flexible to choose an indent depth range, within which reliable hardness value can be obtained. Moreover, the film hardness seems to be independent of the film thickness or ALD cycles, indicating a homogeneous structure throughout the film bodies. The reason for the exceptional behavior of the 50 nm thick film is unclear. However, it is noticed that this film is also the hardest one among all at each depth range.

The validity of the measured hardness is further verified by comparing it to the indentation results of an ALD Al_2O_3 film on sapphire, a substantially harder substrate. It is seen that for a 300 nm thick ALD Al_2O_3 film deposited on silicon and sapphire substrates the hardness is fairly similar over a contact-depth/film-thickness range of 2–17% irrespective to substrate type and indent depth (Table III). Considering sapphire being significantly harder than silicon (Table IV), the constant hardness suggests that the indenter induced no plastic deformation in the substrates in the related indent depth range. Therefore, the measured hardness is free of substrate effect and reliable.

Based on this study, the 10% rule of thumb normally required in nanoindentation for film hardness without substrate effect can be relaxed on the ALD Al_2O_3 films on single crystal silicon substrate when using a sharp cube-corner indenter. This provides more freedom for indentation procedure design in the case of ultrathin films while surface roughness and high noise-to-signal ratio at shallow indent depths have to be accounted. Here, one should bear in mind that property data from excessive deep indent range should be avoided for the potential pile-up and/or sink-in of surface material around the tip that is more pronounced for film/substrate systems.[17] Material pile-up and/or sink-in may induce error in calculating the contact depth at the peak-load when using the Oliver-Pharr's method.

TABLE II. Measured hardness of the Al_2O_3 films at specific contact depths, GPa.

Film thickness (nm)	Contact depth (nm)				
	4.1–4.7	8.5–12.5	15.5–17.7	49.8–51.7	70.8–76.4
10	14.4 ± 0.6				
20	13.3 ± 0.5	11.9 ± 0.5			
50	13.7 ± 0.4	11.9 ± 0.3	11.7 ± 0.3	12.2 ± 0.7	11.5 ± 0.1
100	13.7 ± 0.7	11.5 ± 0.3	11.1 ± 0.3	10.6 ± 0.1	10.9 ± 0.1
300	13.5 ± 0.7	11.6 ± 0.5	11.1 ± 0.2	10.3 ± 0.1	10.0 ± 0.1
600	13.2 ± 1.0	10.7 ± 0.2	11.1 ± 0.3	10.3 ± 0.1	9.9 ± 0.1

TABLE III. Property comparison of a 300 nm ALD Al_2O_3 film on silicon and sapphire substrates at specific contact depths.

Substrate	Properties (GPa)	Contact depth/film thickness (%)		
		2.8–4.2	5.2–6.0	16.6–17.2
Si	Hardness	11.6 ± 0.5	11.1 ± 0.2	10.3 ± 0.1
	Elastic modulus	181.1 ± 11.9	185.2 ± 10.4	169.0 ± 5.1
Sapphire	Hardness	10.6 ± 0.3	10.9 ± 0.2	10.5 ± 0.1
	Elastic modulus	188.3 ± 8.4	186.0 ± 10.7	200.4 ± 6.2

The measured elastic modulus of the 300 nm thick Al_2O_3 film is also presented in Table III. Here, the modulus values are determined from the reduced modulus or contact modulus, E_r, by using the equation[13]

$$\frac{1}{E_r} = \frac{1-\nu_i^2}{E_i} + \frac{1-\nu_i^2}{E_f}, \tag{3}$$

where E_i and E_f are the elastic modulus of the indenter and the film and ν_i and ν_f are the corresponding Poisson's ratio. For diamond indenter, $E_i = 1141$ GPa, and $\nu_i = 0.07$.[13] The Poisson's ratio of the ALD Al_2O_3 film is taken as 0.24.[6] The changes of modulus value with deeper indents in Table III demonstrate an opposite trend for the two substrates indicating substrate effect. Referring to the elastic modulus values in Table IV, the measured film modulus (Table III) starts to drop if the substrate is silicon and to rise if it is sapphire when the ratio of contact-depth-to-film-thickness is over 17%. This is understandable since as the indenter penetrates deeper into the film the information in the unloading data will be more substrate dominant. From the results in Tables III and IV, one may estimate that the real film modulus should fall between 180 and 190 GPa. For the 300 nm thick film, it requires that the indent depth is less than 18 nm or 6% of the film thickness for minimizing the substrate effects on the measured film modulus. For a 100 nm thick film, the depth should be under 6 nm, which is very challenging for the nanoindentation instrument. Therefore, modeling the whole elastic field under given indentation conditions with the knowledge of interfacial stress between the film and substrate is necessary for obtaining true elastic modulus of thin ALD films.

TABLE IV. Measured mechanical properties of the film-free substrates.

Substrate reference	Properties (GPa)	
Si	Hardness	9.8 ± 0.2
	Elastic modulus	154.8 ± 5.0
Sapphire	Hardness	31.0 ± 0.8
	Elastic modulus	341.8 ± 13.8

IV. SUMMARY AND CONCLUSIONS

In this study, ALD Al_2O_3 films of thickness varying from 10 to 600 nm were deposited on SSP-Si wafer at 300 °C, and the film hardness was measured by nanoindentation. To improve the reliability of nanoindentation hardness measurement of the ALD Al_2O_3 films, the characteristics of the indentation load-displacement response of the substrate reference sample was first investigated. A highly repeatable point of elastic to elastic–plastic deformation transition was observed at a specific and shallow contact depth. The occurrence of this transition correlated to a sharp increase of the power-law exponent, m, when fitting the unloading data to a power-law relation. This sharp increase of m was linked to phase transformation occurring in unloading, a unique phenomenon in single crystal silicon. When indenting the Al_2O_3 films on the silicon substrate, the corresponding m values fell into a narrow region over wide indent depth ranges. This is thought to indicate that the silicon substrate was in an elastic state, or in other words, no plastic deformation occurred in the substrate as the films were indented to the corresponding depths. As a consequence, by carefully monitoring the variation of the exponent "m" when fitting the unloading data from a valid indentation curve to a powder-law equation, film hardness obtained at indentation depths much larger than 10% film thickness may still be treated as reliable true film property free of substrate effects. This enables the use of the conventional Oliver and Pharr's method for quick accessing the hardness of thin films on silicon substrate. From the results of the study, it is concluded that the hardness of the ALD Al_2O_3 films deposited on single crystal silicon can be measured by nanoindentation with good confidence. For films thicker than 20 nm, the hardness is about 11 GPa, independent of film thickness.

ACKNOWLEDGMENTS

This work has been made within the MECHALD project funded by Tekes and Finnish Industries and is linked to the Finnish Centre of Excellence in Atomic Layer Deposition of the Academy of Finland.

[1]R. L. Puurunen, J. Appl. Phys. **97**, 121301 (2005).
[2]M. Ritala and M. Leskelä, *Atomic Layer Deposition Handbook of Thin Film Materials*, edited by H. S. Nalwa (Academic Press, New York, 2002), Vol. 1, pp. 103–159.
[3]S. M. George, Chem. Rev. **110**, 111 (2010).
[4]R. L. Puurunen, H. Kattelus, and Suntola, "Atomic layer deposition in MEMS technology," in *Handbook of Silicon-Based MEMS Materials and Technologies*, edited by Lindroos Veikko, Tilli Markku, Lehto Ari, and Motooka Teruak (Elsevier, New York, 2010), pp. 433–446.
[5]M. K. Tripp, C. Stampfer, D. C. Miller, T. Helbling, C. F. Herrmann, C. Hierold, K. Gall, S. M. George, and V. M. Bright, Sens. Actuators A **130–131**, 419 (2006).
[6]K. Tapily, J. E. Jakes, D. S. Stone, P. Shrestha, D. Gu, H, Baumgart, and A. A. Elmustafa, J. Electrochem. Soc. **155**, H545 (2008).
[7]D. C. Miller, R. R. Foster, S.-H. Jen, J. Bertrand, S. J. Gunningham, A. S. Morris, Y.-C. Lee, S. M. George, and M. L. Dunn, Sens. Actuators A **164**, 58 (2010).
[8]L. Borgese, M. Gelfi, E. Bontempi, P. Goudeau, G. Geandier, D. Thiaudière, and L. E. Depero, Surf. Coat. Technol. **206**, 2459 (2012).
[9]W.-E. Fu, C.-W. Chang, Y.-Q. Chang, C.-K. Yao, and J.-D. Liao, Appl. Surf. Sci. **258**, 8974 (2012).
[10]W.-E. Fu, C.-W. Chang, Y.-Q. Chang, C.-K. Yao, and J.-D. Liao, Thin Solid Films **529**, 402 (2013).
[11]S. Bull, J. Vac. Sci. Technol. A **30**, 01A160 (2012).
[12]A. C. Fischer-Cripps, Vacuum **58**, 569 (2000).
[13]W. C. Oliver and G. M. Pharr, J. Mater. Res. **7**, 1564 (1992).
[14]G. M. Pharr and A. Bolshakov, J. Mater. Res. **17**, 2660 (2002).
[15]N. Schwarzer, Thin Solid Films **494**, 168 (2006).
[16]R. B. King, Int. J. Solids Struct. **23**, 1657 (1987).
[17]R. Saha and W. D. Nix, Acta Mater. **50**, 23 (2002).
[18]S. M. Han, R. Saha, R. Banerjee, G. B. Viswanathan, B. M. Clemens, and W. D. Nix, Acta Mater. **53**, 2059 (2005).
[19]S. M. Han, R. Saha, and W. D. Nix, Acta Mater. **54**, 1571 (2006).
[20]D. L. Joslin and W. C. Oliver, J. Mater. Res. **5**, 123 (1990).
[21]J. Hay and B. Crawford, J. Mater. Res. **26**, 727 (2011).
[22]O. M. E. Ylivaara *et al.*, "Aluminum oxide from trimethylaluminum and water by atomic layer deposition: residual stress, elastic modulus, hardness and adhesion," Thin Solid Films (to be published).
[23]J. Musil, Surf. Coat. Technol. **125**, 322 (2000).
[24]M. Fujikane, S. Nagao, X. W. Liu, D. Chrobak, S. Yamanaka, A. Lehto, and R. Nowak, J. Alloys Compd. **448**, 293 (2008).
[25]I. Aaltio, X. W. Liu, M. Valden, K. Lahtonen, O. Söderberg, Y. Ge, and S.-P. Hannula, "Nanoscale surface properties of a Ni–Mn–Ga 10M magnetic shape memory alloy," J. Alloys Compd. (in press).
[26]T. L. Li, Y. F. Gao, H. Bei, and E. P. George, J. Mech. Phys. Solids **59**, 1147 (2011).
[27]D. Chrobak, N. Tymiak, A. Beaber, O. Ugurlu, W. W. Gerberich, and R. Nowak, Nat. Nanotechnol. **6**, 480 (2011).
[28]V. Domnich and Y. Gogotsi, Rev. Adv. Mater. Sci. **3**, 1 (2002).